An atlas of spectra of B6–A2 hypergiants and supergiants from 4800 to 6700 Å

By: E. L. Chentsov, S. V. Ermakov, V. G. Klochkova, V. E. Panchuk , K. S. Bjorkman, and A. S. Miroshnichenko

Abstract:

We present an atlas of spectra of 5 emission-line stars: the low-luminosity luminous blue variables (LBVs) HD 168625 and HD 160529, the white hypergiants (and LBV candidates) HD 168607 and AS 314, and the supergiant HD 183143. The spectra were obtained with 2 echelle spectrometers at the 6-m telescope of the Russian Academy of Sciences in the spectral range 4800 to 6700 Å, with a resolution of 0.4 Å. We have identified 380 spectral lines and diffuse interstellar bands within the spectra. Specific spectral features of the objects are described.

Key words: stars: emission-line, Be – stars: individual: HD 160529, HD 168607, HD 168625, HD 183143, AS 314

Article:

1. Introduction

This paper presents a comparative description of the optical spectra of several white hypergiants and supergiants. It is an addition to existing spectral atlases such as the atlases of Verdugo et al. (1999), Stahl et al. (1993) and Markova & Zamanov (1995). These results were obtained as part of a study of massive evolved B- and A-type stars with luminosities close to the empirical limit suggested by Humphreys & Davidson (1979). Our study included a search for possible luminous blue variable (LBV) stars within this subset of stars.

The nature of LBVs is well defined in the surveys by Humphreys & Davidson (1994) and van Genderen (2001). During the process of becoming an LBV, a star does not lose the "Alpha Cyg-type microvariability" which is usual in normal super- and hypergiants. Instead, it also begins to show optical brightenings, accompanied by reddening of the optical colors, all while maintaining a roughly constant luminosity. This behaviour could be attributed to an increased strength and density in the stellar wind, which would cause the wind to become opaque in the continuum, thereby creating a pseudo-photosphere; however, a real increase of the stellar radius along with a decrease in the surface temperature cannot be ruled out.

The amplitude of variations in brightness and temperature decrease as the luminosity decreases. In the least luminous LBVs ($M_{bol} \sim -9$ mag), the temperature varies between 12000– 13 000 (the latest B-subtypes) and 7500–8000K (the earliest A-subtypes).

The least luminous LBVs are quite rare; only 2 of them have been identified in the Milky Way thus far (van Genderen 2001). Both of these objects are included here (HD 168625, B6 Ia^{+} and HD 160529, B 8–A3 Ia^{+}) along with 2 additional LBV candidates (HD 168607, B9 Ia^{+}, and AS 314, A0 Ia), and the supergiant HD 183143, B7 Ia. HD 168625, HD 168607, and HD 160529 have almost the same luminosity ($M_{bol} \sim -9.1$ mag), while the remaining 2 objects are ~1 mag less luminous. In the Hertzsprung-Russell diagram, HD 168625 is located in the lower part of the inclined instability strip, where LBVs are located during their brightness minima, while HD 160529 is located in the vertical strip, corresponding to LBVs brightness maxima and coinciding with the "yellow void" (Nieuwenhuijzen & de Jager 1995). The evolutionary history and current evolutionary state are reasonably understood only for HD 168625 (Nota et al. 1996) and HD 160529 (Sterken et al. 1991). Both these stars have apparently passed the red supergiant phase and lost most

of their mass. In the case of HD 168625, an enhanced nitrogen abundance in both the atmosphere and the circumstellar material favors this conclusion (Nota et al. 1996; García-Lario et al. 2001).

A detailed comparison of the spectra of the stars included in this study with each other, and with spectra of other objects, may help in a search for new spectroscopic criteria to distinguish LBVs from either quasistationary hypergiants or lower-mass supergiants at the post-AGB stage. In this connection (and intrinsically), one spectroscopic feature of the stellar wind is particularly interesting. The broad P Cygni-type absorptions can have moving local depressions, which appear initially at the red edge of the absorption component and later move to the blue edge (these are known as "discrete absorption components", or DACs). This effect was first noted in the only LBV in the northern sky, P Cygni (Markova 1986). Since then, it has been observed in hypergiants earlier than B2 (Fullerton et al. 1992; Rivinius et al. 1997) and later than B9 (Chentsov 1995; Kaufer et al. 1996). We believe that HD 168625 and HD 183143 are objects which may fill the gap in the late B-type stars.

In Table 1 we present our estimates of the spectral types and absolute visual magnitudes of the objects, along with their optical brightness, galactic coordinates, and dates of the observations. HD 183143 is located between the local (relative to the Sun) spiral arm of the Milky Way and the adjacent interior (Sagittarius–Carina) arm, while the other objects belong to the latter.

2. Observations and data reduction

The spectra were obtained at the 6-m telescope of the Special Astrophysical Observatory (SAO) of the Russian Academy of Sciences using 2 echelle-spectrometers, PFES (Panchuk et al. 1998) and LYNX (Panchuk et al. 1999). PFES is mounted in the prime focus cage and is equipped with a CCD detector of 1160 x 1040 pixels, each 16 x 16 μm in size. It provides a spectral resolving power of $R \sim 15\,000$ in the range 4500– 7930 Å. LYNX is mounted in a Nasmyth focus and, with the same CCD, provides $R \sim 25\,000$ in the range 4725–6325 Å.

Parts of the spectra included in the atlas are limited to the range between 4800 and 6700 Å due to a significant sensitivity reduction of the CCD shortward of this range and effects of the atmospheric and interstellar extinction, and to the wide telluric bands affecting the spectra longward of it. The signal-to-noise ratio in the chosen spectral range for all the spectra shown in this atlas is higher than 100. Combined with the spectral resolving power, this allowed us not only to detect rather weak lines but also to study their profiles.

The 2D spectra were reduced (applying standard procedures of bias subtraction, scattered light and cosmic ray trace removal, and order extraction) using the task ECHELLE under MIDAS (version 1998). Further measurements (photometric and positional) in the 1D spectra were made in the DECH20 package (Galazutdinov 1992). In particular, positions of the spectral lines were measured by matching the original and mirrored profiles. Instrumental corrections for the measured wave-lengths were derived using telluric lines of oxygen and water. Special care was taken deriving these corrections in the spectra obtained with PFES, which is mechanically and thermally less stable than LYNX. The residual systematic errors, estimated using the interstellar lines of Na I and K I, do not exceed 2kms^{-1}. The laboratory wavelengths, used to measure radial velocities (RV), were taken from tables of Striganov & Odintsova (1982), Johansson (1978), and Chentsov et al. (1996). The diffuse interstellar bands (DIBs) are very strong in the spectra of our objects. The broadest of them (e.g., at 4820, 4880, and 4970 Å) are poorly seen in echelle spectra, be-cause they occupy most of the corresponding order width. On the other hand, there are many DIBs (e.g., at 5780, 5797, and 5850 Å) which have widths comparable to those of stellar absorption lines. We measured RVs of only the latter DIBs using the atlas of Galazutdinov et al. (2000).

3. Atlas and list of identified spectral lines

The spectra of all 5 stars in the range 4800–6700 Å are presented in the form of intensities, normalized to the continuum, versus laboratory wavelengths. The atlas is divided into sections 120 Å in width. As an example, the fragment within the spectral region λ4990–5110Å is shown in Fig. 1. The atlas in whole is enclosed. In each section, the objects are shown in the same order as in Table 1, i.e. with the effective temperature decreasing from top to bottom. The emission peaks of Hα and Hβ were truncated because they

were distorted by saturation. Selected strong lines in the top and bottom spectra are marked in each section of the atlas. In addition, DIBs are indicated by circles above the upper spectrum. Numerous atmospheric telluric lines also are present but are not marked.

These spectra were not obtained specifically for this atlas. As seen from Table 1, we have used several spectra, obtained at different times and with different spectrometers, for 4 out of the 5 objects. The atlas shows averaged spectra of these objects. The RVs and profiles of some lines vary with time. For this reason (and for the purpose of this atlas), we have chosen to use the spectra with minimal differences in line profiles with respect to each other in order to demonstrate the characteristic profiles of these lines. We selected spectra for averaging in which the profile shape variations do not exceed 2% of the continuum level, except for the lines of hydrogen, the strongest lines of Fe II, and a few others (some examples can be seen in Figs. 3 and 4).

The list of 380 identified stellar, circumstellar, and interstellar lines and DIB s is presented in Table 2. Multiple narrow telluric lines detected in the spectra are not listed in the table. High-excitation Fe II absorption lines are marked simply with a letter "h" instead of the multiplet number. Any line found in the spectrum of an object is listed in the corresponding column with the residual central intensity normalized to the continuum (r); this is used instead of the usual equivalent width to make searches for lines in the atlas easier. In the case of a blend, the value listed is for the stronger component. For example, the list shows N II (Mult. 19) 5001.3 Å in HD 183143 and Fe II 5001.9 Å in HD 168607. For P Cyg-type profiles we list extreme values of both the absorption and emission components. The weakest of the detected lines have $r = 1 \pm 0.01$. There are a few cases of larger measurement errors where only one digit is quoted for the central intensity r (for example, H-beta in AS314 and HD160529).

In the spectra of HD 168625 and HD 183143, which showed primarily pure absorption spectra, the lines were identified according to our measured RVs and relative intensities. These spectra were then used as templates for identifying lines in the other sample objects, where the features were somewhat more complex. About 20% of the lines in the spectra of HD 168607 and AS 314 were emission lines. In the spectrum of HD 160529, emission lines were less common, but most of the absorption lines were split into several components. The specific shapes of the line profiles are indicators of the atmospheric expansion and the presence of a RV gradient. They can also be used as additional criteria for line identification.

Table 1. Main parameters of stars studied.

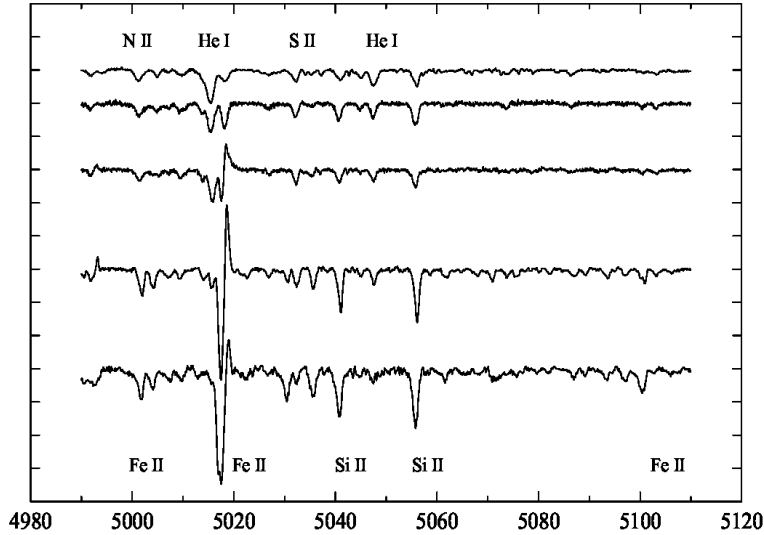| Star	Sp	M_v	V	l	b	Date	*
HD168625	B6 ia$^+$	−8.5	8.4	15	−1.0	1998 June 19	(P)
						1999 June 4	(L)
						2000 June 24	(L)
HD183143	B7 ia	−7.7	6.9	53	0.6	1999 June 5	(L)
						2001 June 7	(P)
HD168607	B9 ia$^+$	−8.8	8.3	15	−1.0	1999 June 19	(P)
						2000 June 24	(L)
						2001 June 4	(P)
AS 314	A0 ia	−7.5	9.8	19	−3.7	1999 June 30	(L)
= V452 Sct						2000 July 5	(P)
						2001 June 4	(P)
HD160529	A2 ia$^+$	−8.9	6.6	356	−1.7	2001 June 4	(P)

* P = PFES; L = Lynx.

Fig. 1. *An example page of the spectral atlas. The spectra are shown in the following order from top to bottom: HD 168625, HD 183143, HD 168607, AS 314, and HD 160529. The intensities (ordinates) are in continuum units with tick mark intervals of 0.2. The wavelengths (abscissas) are in Å.*

Weak lines are dominant in the spectra of late-B subtypes. In our list the fraction of absorptions with $r \geq 0.9$ is about 90% for HD 168625, HD 183143 and HD 168607, 85% for AS 314, and 75% for HD 160529. In the spectrum of the hottest of our stars, HD 168625, we found lines of H I, He I, C II, N I, O I, Ne I, Al III, Si II, Si III, S II, Fe II, and Fe III. In the spectrum of the coolest star, HD 160529, some of these lines are also seen, but lines of N I, Na I, Mg I, Mg II, Al II, Sc II, Ti II, Cr II, Mn II, Fe I, and Ba II are present instead of C II, N II, Al III, Si III, and Fe III.

4. Spectroscopic features of the objects

As mentioned above, all the objects are more or less spectroscopically variable; the line profile shapes and *RV*s change differently with time. We have grouped together most of the lines (or their components) which either have a constant *RV* or a *RV* which gradually changes along with the line intensity. The mean *RV*s for some of these groups are collected in Table 3, where each object is represented by one spectrum with the observing date listed (the same spectra are presented in Fig. 2 as well). A description and comparison of the numerous spectra we have for each individual star is beyond the scope of this paper and will be presented elsewhere. The note $r \rightarrow 1$ indicates that the listed *RV* value is that which the absorption line (or absorption component of the P Cyg-type profile) approaches as the value of r increases (or as the depth of the line decreases). In other words, it corresponds to the *RV*s of the weakest absorption lines or components. For emission lines in P Cygni features, r is defined by the residual intensity of the blueshifted absorption component adjacent to the actual emission peak. The limit $r \rightarrow 1$ corresponds to the case where there is no blueshifted absorption, and the feature appears as a single emission line. Below we discuss typical features of the spectrum of each object.

4. 1. HD 168607

HD 168607 has the most interesting and best studied spectrum. It has been described by Chentsov & Luud (1989) and Chentsov & Musaev (1996). One can nicely see its features comparing the spectra of HD 168607 and HD 183143 in Fig. 1 and other sections of the atlas. Differences in the intensity and profile shape are small not only in the He I and light element lines, but also in those Fe II absorptions with low level excitation potentials of more than 10 eV (note that this group is referred to as "Fe II high ex." in Table 3 and Fig. 2). At the same time, these Fe II lines and the strong absorptions of Si II (2) in the spectrum of HD 168607 are blueshifted by ~12 km s^{-1} with respect to the He I and light element lines (see Table 3 and Fig. 2a). Since the Fe II and Si II (2) lines are formed in the atmosphere above those of the light elements, this differential shift can be interpreted as evidence that the corresponding atmospheric layers are expanding.

Relations between the *RV*s and r values for HD 168607 are shown in Fig. 2a. Large filled circles, which represent individual absorption lines or absorption components of P Cyg profiles, form several horizontal sequences. The upper sequence represents pure (photospheric) absorption lines of He I, C II, etc. In the range

$0.75 \le r \le 0.98$, they give a mean $RV = 11$ km s^{-1}, with a scatter due to measurement errors only. As mentioned above, the strong Si II 6347 Å line and the weak Fe II high excitation lines have lower RV values.

The other horizontal sequences represent discrete components, in which the absorption parts of the P Cyg-type profiles are split, in the Hα and Fe II lines with low excitation potentials of the low levels (~3 eV). These are strictly horizontal; the RVs are independent of r. The upper of these sequences ($RV = -14$kms^{-1}) relates to the deepest wind components of the Fe II lines; it is not observed in the Hα due to strong emission at this RV. The other two sequences ($RV = -75$ and -120 km s^{-1}) include weak components of the Fe II lines and strong components of the Hα. This effect is also illustrated in Fig. 3a, where the profiles of 2 lines of Fe II with different intensities are compared.

Table 3. Average heliocentric radial velocities $\overline{RV}$ (km s^{-1}).

Name(HD)	168625	183143	168607	AS314	160529
Date	1999 June 4	1999 June 5	1995 June 18	2000 July 5	2001 June 4
Emission lines/components ($r_{absorption} \to 1$)					
				10	−60
Absorption lines/components					
He I, S II,... (r → 1)	17	11	11	−43	−28
Fe II high ex.			0	−40	−30
Si II (2)	12	13	−2	−52	−26
Fe II low ex. (r → 1)			−15	−102	−14
					−60
					−104
Fe II (42) 4923, 5018, 5169	12	13	−14	−106	−75
			−75		−104
			−120		
Hα	−35	−47	−75	−112	−105
	−105		−120		
Abs. I.S.					
Na I (1)	1	0		−5	−14
DIB	10	−3	8	−7	−6

The picture described is not characteristic of hot luminous stars with strong winds. For example, a gradual increase of the RV of the absorption components of P Cyg-profiles with increasing r is noticed in the spectrum of P Cyg, a prototype of such stars (de Groot 1969). The same effect is observed in AS 314 (see Sect. 4.4 and Fig. 2b). Perhaps in the case of HD 168607 there is an asymmetric wind, or multiple detached envelopes with different expansion velocities and small radial velocity gradients. Thus, a spectroscopic monitoring of HD 168607 is highly desirable.

Figure 3a also shows how the profiles of different lines are changing with time. While the photospheric absorption of He I and the emission parts of the Fe II line profiles changed a little, the wind absorption components of the latter redistributed completely. In our data, they were found at any position between - 10 and -140 km s^{-1}.

As the absorption components of the lines with P Cyg profiles become weaker, the RVs of their emission peaks approach the mean value for the symmetric stationary emissions of Fe II (z^4D–c^4D) (marked with plusses in Fig. 2a). The latter do not show variations of shape, intensity or RV with time. They are probably formed in extended spherically-symmetric envelopes.

The corresponding mean RV, 10 km s^{-1}, is listed in the first line of Table 3 and is adopted as the RV of the star's center of mass.

4.2. HD 168625

This star is considered an LBV because of its circumstellar envelope, gaseous and dusty components of which have been described in detail by Hutsemekers et al. (1994), Nota et al. (1996), and Robberto & Herbst (1998). However, neither photometry (van Genderen et al. 1992; Sterken et al. 1999) nor spectroscopy (Chentsov & Luud 1989; Nota et al. 1996) revealed any of the LBV features in this star. As seen in Fig. 1, in other sections of the atlas and Table 2, the spectrum of HD 168625 is very similar to that of HD 183143. Differences, which are illustrated by blends of He I–Fe II at 4922/24 and 5015/18 Å, reflect only the temperature difference. In our spectral region significant profile variations are seen only in the hydrogen lines. Their RVs also vary significantly (by tens of km s^{-1}) with time and from line to line (Balmer progression). For other lines, the amplitudes of the temporal variations and differential shifts are limited to a few km s^{-1}. Since the relevant information is contained in Table 3, we do not show a plot similar to Fig. 2 for HD 168625. The absorptions of He I, C II, N II, Al III, Si III, S II, and Fe III, whose intensity maxima are reached in B2–5 spectral types, have RVs very close to each other and are grouped together (hereafter, the He I lines and others). The weakest of these are formed in the deepest photospheric layers of HD 168625 reachable with our spectral resolving power. Table 3 lists the RV of these lines obtained on 1999 June 4 (+17 km s^{-1}), while the RVs measured in our other spectra of the object vary between + 8 and + 12 km s^{-1}. The absorptions of S III(2) and Fe II(42) are formed higher in the atmosphere and are usually shifted blueward with respect to the He I lines and others. Apparently, the RV variations are due to atmospheric pulsations, while the line differential shifts are due to atmospheric expansion.

The angular distance between HD 168625 and HD 168607 is only 1 min of arc, and both stars are located in the vicinity of the M 17 nebula. Hence, their close position is hardly accidental. Nevertheless, there are suggestions that the distance to HD 168625 is much smaller (Robberto & Herbst 1998) or larger (Hutsemekers et al. 1994) than that to HD 168607. The latter argument was based on RV differences. Our data show that the mean RV for the deep photospheric layers (which is close to the value for the star itself) is the same for both stars within the measurement accuracy, + 10 ± 2 km s^{-1}. The RVs derived from the DIBs and the velocity for the whole complex (M 17–Ser OB1) are close to this value. This suggests that both stars belong to this complex (Chentsov & Luud 1989).

The Hα profiles, obtained in 1997, 1998, and 1999, are shown as relationships of r vs. RV in Fig. 4. Similar profiles were also observed in 1995 (Nota et al. 1996). The position of the red wing of the Hα emission component varies a little with time. The averaged part of the profile for $RV \geq 100$ kms^{-1}, mirrored with respect to the star's mean RV, is shown by a dotted line in Fig. 4. We see that a significant part of the emission component is hidden by the strong and variable wind absorption. Are we dealing with moving DACs as mentioned in Sect. 1? Figure 4 does not contradict this suggestion, but the question remains open as HD 168625 is not observed frequently enough.

4.3. HD 183143

As for HD 168625, we do not plot the RV vs. r dependencies. The pulsations and RV gradients in the atmosphere of HD 183143 are almost the same as in HD 168625, but the wind absorption components of the hydrogen lines are significantly weaker. This can be clearly seen comparing Figs. 4 and 5. The hydrogen line profiles, obtained in May–August 1997 by G. A. Galazutdinov and F. A. Musaev with a coudé spectrometer at the SAO 1-m telescope (with spectral resolving power $R = 45\,000$), are shown in Fig. 5. The parts of the profiles that are not affected by absorption allow us to estimate the star's RV. It is based on the bisector of this parts of the line. Their centre, marked by a dashed line in Fig. 5, corresponds to + 15 km s^{-1}. This value is close to that obtained for the stationary emissions of Fe II in the near-IR region (7496 Å, 7513 Å and others; see Johansson 1977). It also fits within the range of RVs that we derived for the weakest absorptions (9–18 km s^{-1}). The blue parts of the hydrogen profiles in Fig. 5 apparently reflect other phases of the absorption component motion within RVs from −10 to −110 km s^{-1}. However, to prove the existence of these motions, more frequent (perhaps weekly) observations would be needed.
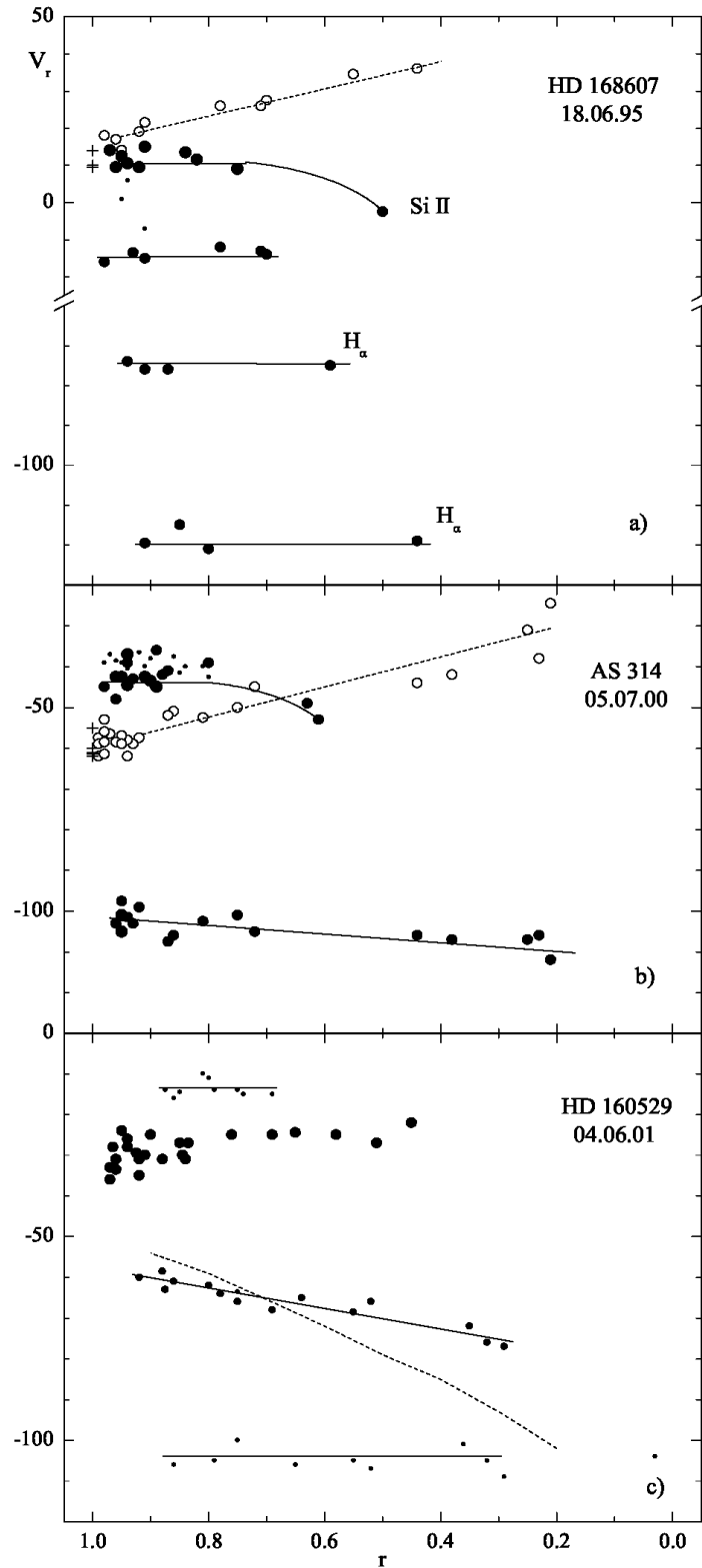
Fig.2. *Relationships between the RVs (km s^{-1}) and central residual intensities of the absorption lines and absorption components of P Cyg-type profiles in the spectra of HD 168607 (panel a)), AS 314 (panel b)), and HD 160529 (panel c)). Each symbol represents a separate line or component. In panels a) and b), large filled circles represent absorption lines or components; small filled circles represent high-excitation absorption lines of Fe II; open circles represent emission components; and pluses represent Fe II lines with pure emission. In panel c), large filled circles represent lines of He I, S II, and high-excitation Fe II lines; small filled circles and dots represent the main and secondary components of low-excitation Fe II lines. The lines show linear fits to the relationships. The dashed line in panel c) shows the dependence of the RVs of the gravity centre of the entire profile, based on the relative intensities of the low-excitation Fe II lines.*
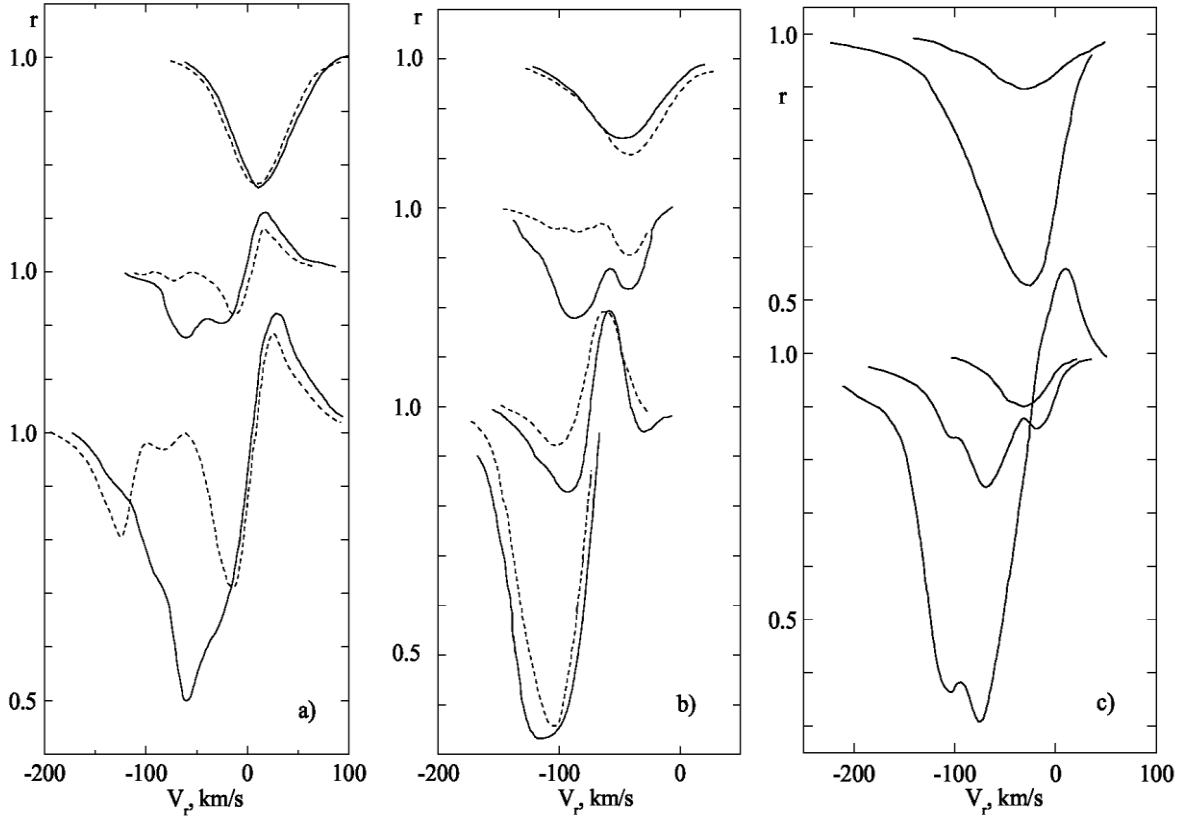
Fig. 3. a) *Line profiles in the spectra of HD 168607 obtained on 1992 August 14 (solid lines) and on 1995 June 18 (dashed lines). From top to bottom: He I (11) 5876 Å, Fe II (49) 5276 Å, Fe II (42) 5169 Å.* **b)** *Line profiles in the spectra of AS 314 obtained on 2000 July 5 (dashed lines) and on 2001 June 4 (solid lines). From top to bottom: He I (11) 5876 Å, Cr II (30) 4824 Å, Fe II (48) 5363 Å, Fe II (42) 5169 Å (absorption part only).* **c)** *Line profiles in the 2001 June 4 spectrum of HD 160529. From top to bottom: He I (11) 5876 Å, Si II (30) 6347 Å, Fe II 5387 Å, Fe II (48) 5363 Å, Fe II (42) 5018 Å.*

4.4. AS 314

The spectral features of AS 314 have been described by Miroshnichenko et al. (2000). As seen in Fig. 1, in the atlas and in Table 2, the pure emission and P Cyg-type profiles include the same lines as those in the spectrum of HD 168607. However, the P Cyg-type profile shape in AS 314 is simpler: the absorption components are not split, and they occur at lower velocities (we found the *RV* variations did not exceed 20 km s- 1). Additionally, we find that the P Cyg features of AS314 show a positive emission velocity shift with increasing absorption component depth (like HD 168607) and a negative absorption velocity shift with increasing absorption depth (unlike HD 168607) (Fig. 2b). Nevertheless, some absorption profiles of moderate intensity are more complex. For example, the Cr II (30) lines look split into 2 components, like those in spectroscopic binaries with 2 visible spectra. The components' depths and intensity ratio change with time (Fig. 3b). However, the profiles' total widths remain the same, while the *RV*s of the red and blue components remain close to those of the single (not split) absorptions of the He I and others group and of the P Cyg-type absorptions of the weak Fe II lines of low excitation, respectively. As one can see in Fig. 3b, the shape of the Cr II (30) line profiles can be explained by the presence of emission components which do not rise above the continuum, in contrast to the Fe II lines. The *RV*s of these "split' (emission) components coincide with those of the purely emission Fe II lines and of the emission components of the P Cyg-type profiles within the measurement errors (Fig. 3b). As in HD 168607, these emission components are the least variable; their mean *RV*s changed between -50 and -60 km s^{-1} in the 5 spectra we obtained in SAO with the echelle spectrometers in 1997–2001. Probably the star's *RV* is bound within this interval. However, such a *RV* is very unusual for the corresponding line of sight in the Milky Way. We mentioned above that the *RV* of HD 168607 and HD 168625, which are located within just 4 degrees of galactic longitude from AS 314, is +10km s^{-1}. Moreover, among all our objects AS 314 has the largest galactic latitude. Perhaps we are dealing with a runaway star (see Miroshnichenko et al. 2000). We should also note a strong similarity of the spectra of AS 314 and LS 3591, which is probably a low-mass post-AGB star (Venn et al. 1998). Hence, the nature and evolutionary state of AS 314 still need to be studied further.

4.5. HD 160529

This object is somewhat different from the others. The spectroscopic response to instabilities in its atmosphere is much stronger than in HD 168625 and HD 183143, but different from that in HD 168607 and AS 314. In this connection, we again emphasize that the meaning of the symbols in Fig. 2c is different from those in Figs. 2a, b!

The spectroscopic features of HD 160529 have been described by Wolf et al. (1974) and Sterken et al. (1991). The former paper was based on spectra obtained in early 1970's, when the star was in a maximum brightness state and had a spectral type A2/3. The latter paper was based on spectra obtained in 1986 (the star was close to the brightness minimum) and in 1990 (brightness minimum, spectral type B8). Our spectrum suggests a spectral type of A2 ± 1, with the line profiles appearing very similar to those observed by Wolf et al. (1974). Emission components are seen only in the hydrogen lines and in the strongest Fe II lines. They are shifted to the red by strong absorption components (see the line at 5018 Å in Fig. 3c).
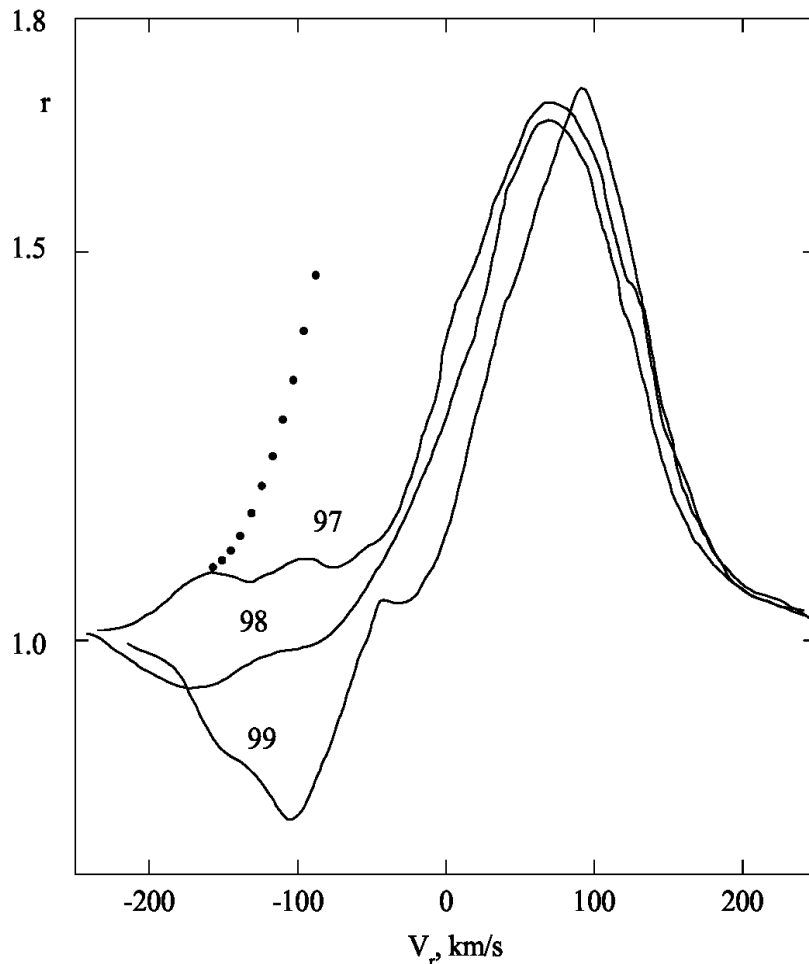

Fig. 4. *The Balmer line profiles in the spectra of HD 168625 obtained on 1997 July 23, 1998 June 19, and 1999 June 4. The dots represent the blue wing position with the absence of the absorption component. The dotted line was derived from the line symmetry assumption (see text).*
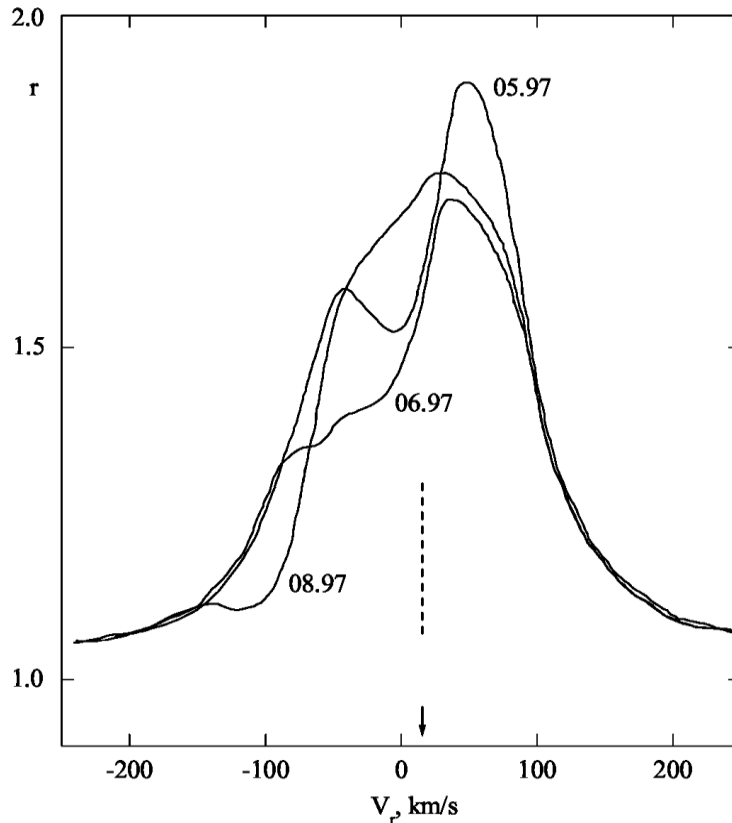
Fig. 5. *The Ha line profile in the spectra of HD 183143 obtained on 1997 May 14, 1997 June 6, and 1997 August 20. The dashed line marks the centre of the symmetric part of the profiles.*

Profiles of the weak absorptions of He I, S II (represented in Fig. 3c by the He I 5876 Å line) and high-excitation Fe II (5387 Å in Fig. 3c) are single and almost symmetric. An asymmetry due to a redshift of the line core with respect to the wings appears in stronger absorptions of N I(3) and Si II(2) (6347 Å in Fig. 3c). Their RVs were measured using the line cores. The shallow slope of the filled circles sequence (corresponding to the absorptions) in Fig. 2c is due to the fact that most of the Fe II lines with $r \geq 0.85$ have a high excitation. They are shifted blueward with respect to the other absorptions (Table 3).

In profiles of the low excitation Fe II lines one can distinguish at least three components: the main component, which is blueshifted with respect to the He I and others, and 2 weaker components, one in each wing (they form the two horizontal sequences in Fig. 2c at -13 and -105 km s^{-1}. The weaker components are clearly recognizable and suitable for measurements in lines of a moderate intensity. However, as the line strengthens, the blue component becomes deeper, while the red one becomes flatter and occupies that part of the profile where the intensity gradient is the largest. As a result, the profile's gravity centre is shifted to the blue (the dashed line in Fig. 2c shows this trend). This is seen when comparing the 5363 and 5018 Å Fe II lines in Fig. 3c. After Sterken et al. (1991), we believe that the closest RV to that of the star's centre of mass (systemic velocity) is the RV determined for the red components of the split Fe II lines (our value is -14 km s^{-1}). Only these lines can be considered photospheric. Others have to be attributed to the wind base and its higher layers.

5. Summary

In this atlas we compare spectra of a set of B6–A2 stars of very high luminosities. The spectral features were carefully found and identified in the range 4800–6700 Å. Previously only an atlas of one star from our list, HD 183143, has been published (Jenniskens & Desert 1994; Galazutdinov et al. 2000), while only small sections of the spectra of the other objects have been presented in different papers.

Since all the stars are variable (especially LBV candidates), our atlas is useful as it presents their spectra at certain epochs. Additionally we have found some new features of the objects. In particular, our spectra suggest that HD 168625 (B6 Ia$^+$) and HD 183143 (B7 Ia) could be considered as candidate objects showing "blueward migrating DACs" (e.g., Markova 2000). We also suggest a new explanation for the complicated

shape of the absorption line profiles in the spectrum of AS 314. Apparently their splitting is due to superposition of narrow emission peaks which are formed in the extended envelope of the star.

References

Chentsov, E. L. 1995, Ap&SS, 232, 217
Chentsov, E. L., & Luud, L. S. 1989, Astrofizika, 31, 5
Chentsov, E. L., & Musaev, F. A. 1996, Astron. Lett., 22, 589
Chentsov, E. L., Musaev, F. A., & Galazutdinov, G. A. 1996, Bull. Spec. Astrophys. Obs., 39, 101
Fullerton, A. W., Gies, D. R., & Bolton, C. T. 1992, ApJ, 390, 650
Galazutdinov, G. A. 1992, Prepr. of the Spec. Astrophys. Observ., No. 92
Galazutdinov, G. A., Musaev, F. A., Krelovski, J., & Walker, G. A. H. 2000, PASP, 112, 648
García-Lario, P., Sivarani, T., Pathasarathy, M., & Manchado, A. 2001, in Post-AGB Objects as a Phase of Stellar Evolution, ed. R. Szczerba, & S. K. Gorny (Kluwer Acad. Publ.), 309
de Groot, M. 1969, Bull. Astron. Inst. Netherlands., 20, 225
Humphreys, R. M., & Davidson, K. 1979, ApJ, 232,409
Humphreys, R. M., & Davidson, K. 1994, PASP, 106, 1025
Hutsemekers, D., van Drom, E., Gosset, E., & Melnick, J. 1994, A&A, 290,906
Jenniskens, P., & Desert, F.-X. 1994, A&AS, 106, 39
Johansson, S. 1977, MNRAS, 178,17P
Johansson, S. 1978, Phys. Scr., 18, 217
Kaufer, A., Stahl, O., Wolf, B., et al. 1996, A&A, 305, 887
Markova, N. 1986, A&A, 163, L3
Markova, N. 2000, A&AS, 144, 391
Markova, N., & Zamanov, R. 1995, A&AS, 114,499
Miroshnichenko, A. S., Chentsov, E. L., & Klochkova, V. G. 2000, A&AS, 144,379
Nieuwenhuijzen, H., & de Jager, C. 1995, A&A, 302, 811
Nota, A., Pasquali, A., Clampin, M., et al. 1996, ApJ, 473, 946
Panchuk, V. E., Najdenov, I. D., Klochkova, V. G., et al. 1998, Bull. Spec. Astrophys. Observ., 44, 127
Panchuk, V. E., Klochkova, V. G., Najdenov, I. D., et al. 1999, Prepr. Spec. Astrophys. Observ. No. 139
Rivinius, Th., Stahl, O., Wolf, B., et al. 1997, A&A, 318, 819
Robberto, M., & Herbst, T. M. 1998, ApJ, 498, 400
Stahl, O., Mandel, H., Wolf, B., et al. 1993, A&AS, 99,167
Sterken, C., Gosset, E., Juettner, A., et al. 1991, A&A, 247, 383
Sterken, C., Arentoft, T., Duerbeck, H. W., & Brogt, E. 1999, A&A, 349,532
Striganov, A. R., & Odintsova, G. A. 1982, Tables of spectral lines of atoms and ions (Moscow, Energoizdat)
van Genderen, A. M. 2001, A&A, 366, 508
van Genderen, A. M., van den Bosch, F. C., Dessing, F., et al. 1992, A&A, 264, 88
Venn, K., Smartt, S. J., Lennon, D. J., & Dufton, P. L. 1998, A&A, 334,987
Verdugo, E., Talavera, A., & Gomez de Castro, A. I. 1999, A&AS, 137,351
Wolf, B., Campusano, L., & Sterken, C. 1974, A&A, 36, 87